Study of Bell Nonlocality in the Minimal Triangle Scenario

Author: Matías Viner Tesoriere.
Facultat de Física, Universitat de Barcelona, Diagonal 645, 08028 Barcelona, Spain.[*]

Advisors: Antonio Acín[1], Bruno Julià-Díaz[2].[†]

Abstract: The study of quantum networks continues to prove its value both in practical and theoretical applications. Among these networks, one of the simplest to consider is the minimal triangle scenario, for which it is not known whether it accepts a quantum nonlocal distribution. To study this, we propose an algorithm based on inflation techniques. Despite promising results, we have not found such a distribution. The code's flexibility also allowed us to explore a subset of symmetric distributions for the three-outcome case, improving some previous results from the field.

I. INTRODUCTION

Indeterminacy in nature is a core tenet of quantum physics. The proof of this fundamental principle came thanks to the efforts of John Bell, who was the first to show that the ability to recover a deterministic model in a certain setup can be experimentally falsified [1]. Consequently, phenomena that falsify determinism are termed *Bell Nonlocality*.

Bell's scenario involved two distant parties performing independently chosen two-output measurements on a shared quantum state. Recent research has focused on generalizing Bell's scenario by increasing the number of parties and shared quantum states, and exploring various connections among parties. This study of quantum networks offers insights into quantum mechanics, robust certification of quantum devices' functioning, and constraints on possible physical theories [2, 6].

When studying such networks, our goal is to investigate if a *quantum-classical gap* exists for a given causal structure. That is, can measurements performed on entangled quantum sources generate correlations that classical physics cannot explain?

A particularly intriguing and seemingly simple network is the *triangle scenario* [3] (see Fig. 1), featuring three parties – Alice, Bob and Charlie – in a triangle-shaped structure. When the parties have binary measurement output, it is known as the *Minimal Triangle Scenario* (MTS). Remarkably, whether a quantum-classical gap exists for the MTS is still an open question. To try to see if such a gap exists is the main focus of this thesis.

The non-convex nature of the correlation set in the MTS makes this problem particularly challenging. We have tackled this problem with the help of *inflation* [7, 8], an algorithm which tests for causal compatibility between a causal structure and a joint probability distribution.

[*] mvinervi7@alumnes.ub.edu

[†] [1]ICFO – Institut de Ciencies Fotoniques, The Barcelona Institute of Science and Technology, 08860 Castelldefels (Barcelona), Spain; [2]Department d'Estructura i Constituents de la Matèria and Institut de Ciències del Cosmos, Universitat de Barcelona, E–08028 Barcelona, Spain

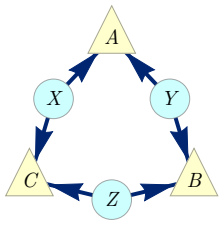

Figure 1: Representation of the triangle scenario. The parties (triangles) are named A, B, C and the resources they share (either local variables or entangled quantum states) are labelled X, Y, Z. Adapted from [8].

II. THEORETICAL FRAMEWORK

A. Bell Nonlocality

Experimental setups in physics laboratories to check for Bell Nonlocality are called *Bell Tests*, and are typically introduced as games involving different parties. In the MTS (see Fig. 1), these tests involve three parties – Alice, Bob, and Charlie – who, after agreeing on a strategy, are separated to produce outputs a, b, c, respectively. They use different processes X, Y, Z to produce these outputs, relying either on classical strategies or by performing local measurements on shared quantum states.

We can mathematically describe the joint probability distribution $P(a, b, c)$ in the classical (or local) case as

$$P(a,b,c) = \int dX\, dY\, dZ\; P_A(a|X,Y) P_B(b|Y,Z) P_C(c|X,Z). \tag{1}$$

The goal is to determine whether a joint $P(a, b, c)$ is local (can be decomposed as in Eq. (1)).

Quantum mechanics introduces a novel nonlocal resource: quantum entanglement. Formally, a joint distribution is *quantum realizable* if there exist states ρ_{AB}, ρ_{BC}, and ρ_{AC}, and *measurements* $\mathcal{M}_A$, $\mathcal{M}_B$, and $\mathcal{M}_C$ such that:

$$P(a,b,c) = \mathrm{tr}\left(\rho_{AB} \otimes \rho_{BC} \otimes \rho_{AC}\; \Pi_a \otimes \Pi_b \otimes \Pi_c\right) \tag{2}$$

for all a, b, c, (this assumes states and measurements are

independent). By measurements we mean the following. Let m_A be Alice's number of outputs. We consider a family of m_A operators,

$$\mathcal{M}_A = \{\Pi_a,\ a = 1, \dots m_A\},$$

where $\mathcal{M}_A$ is a positive operator-valued measure (POVM)[1]. These operators Π_a are positive semidefinite and act on Alice's Hilbert space $\mathcal{H}_A$, satisfying

$$\sum_a \Pi_a = \mathrm{Id}.$$

Similarly, we define POVMs $\mathcal{M}_B$ and $\mathcal{M}_C$ for Bob and Charlie.

B. Certificates of infeasability

Let $\{k_x : x = 1, \dots, N\}$ be a set of measurements outcomes associated with operators $\{K_x : x = 1, \dots, N\}$. Our task is to determine if a quantum state ρ, considered as a density operator, can explain these measurements outcomes. Since ρ is a quantum state, it must be a positive semidefinite operator[2] with unit trace. This problem can thus be expressed as:

$$\begin{aligned} &\text{minimise} && \delta \\ &\text{subject to} && k_x - \delta \leq \mathrm{tr}(K_x\rho) \leq k_x + \delta,\ \forall x \\ &&& \mathrm{tr}(\rho) = 1, \rho \succeq 0. \end{aligned} \tag{3}$$

This is an example of a semidefinite program (SDP), an optimization problem with linear constraints on operators. If the optimal value is $\delta^* = 0$, then the problem is feasible, that is, there exists a quantum state and a POVM compatible with the observed measurement outcomes; if $\delta^* > 0$, we say the problem is infeasible. Each SDP has a corresponding *dual* SDP, derived using a Lagrangian (see [4]). Under mild conditions, the optimal values of both the primal and dual SDPs are equal. It is dual in the sense that if the original SDP was a minimization problem, the dual is a maximization SDP, and vice versa.

It can be proven that the dual of the problem (3) is

$$\begin{aligned} &\text{maximise} && z + \vec{t}\cdot\vec{k} \\ &\text{subject to} && z\cdot\mathrm{Id} + \vec{t}\cdot\vec{K} \preceq 0 \\ &&& \sum_{x=1}^{N} |t_x| \leq 1. \end{aligned} \tag{4}$$

Where we have introduced the vectors $\vec{k} = (k_1, \dots, k_N)$ and $\vec{K} = (K_1, \dots, K_N)$. Now, let ρ be an arbitrary quantum state. Then, for any dual feasible variables $z, \vec{t}$, we have

$$z + \sum_{x=1}^{N} t_x\,\mathrm{tr}(\rho K_x) = \mathrm{tr}\left(\rho\left(z\cdot\mathrm{Id} + \vec{t}\cdot\vec{K}\right)\right) \leq 0. \tag{5}$$

The first equality follows from the linearity of the trace operator and the inequality from the positive definiteness of ρ and the constraints in (4). Therefore, if we find dual feasible variables $z, \vec{t}$ such that $z + \vec{t}\cdot\vec{k} > 0$ for the given measurements $\vec{k}$, then those measurements cannot originate from a quantum state, providing a certificate of infeasibility. Geometrically, the dual SDP provides a *separating hyperplane* in the space of all possible measurements.

C. Inflation

Inflation [7] examines correlations in causal scenarios involving latent nodes (e.g., sources of classical randomness or quantum states) and visible nodes (random variables from measurements). Arrows show the influence direction between systems, specifying system distribution among parties. To avoid causal paradoxes, these arrows must form directed acyclic graphs (DAGs). Figure 2 presents examples of inflations in the triangle scenario.

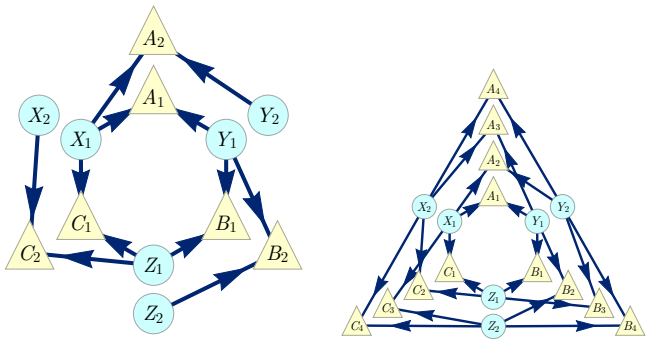

(a) (b)

Figure 2: Two inflations of the triangle scenario: its *spiral* (a) and *web* (b) inflation. Triangles represent observable nodes and circles latent ones. Adapted from [8].

Inflation analyzes distributions in a causal scenario using a hypothetical experiment with multiple copies of latent (physical systems) and visible (operations) nodes in the DAG. Parents of a visible node's copy are copies of the original node's parents, simplifying the characterization of compatible distributions. Constraints on distributions in inflated scenarios become necessary constraints for the original scenario. Thus, inflation discards nonlocal behavior by proof by contradiction: begin by assuming the distribution is local. If it is, it must satisfy the new constraints imposed by the inflated scenario. If it does not, we can conclude that the distribution is nonlocal. Note also that inflation does not allow us to prove

[1] Analogously to how density operators generalize pure states, we can define general measurements that allow for the existence of noise in our systems. A particular instance of this are POVMs, which represent cases where we do not care about the state of our system after the measurement.

[2] For operators A, B, $A \succeq B$ iff $A - B$ is positive semidefinite.

that a distribution is local (it is not an 'if and only if' statement).

Probability distributions in inflation scenarios can be characterized using linear programming for classical or generalized physical systems. Efficient algorithms are available to solve these problems using standard computing resources [8].

III. CODE IMPLEMENTATIONS

Algorithm 1: Finding a Quantum Nonlocal Distribution in the MTS

```
while We have not found a quantum nonlocal distribution do
    Sample a random distribution;
    if Inflation cannot discard locality then
        Return to Step 2;
    else
        Extract the certificate C;
        Minimise C[P_Q], for P_Q ∈ Q; starting from a random quantum distribution;
        Test whether the final distribution is local using inflation;
```

The main goal of this thesis is to determine whether quantum nonlocal behaviour exist in the MTS[3]. Formally, this asks if there are shared states $\rho_{AC}, \rho_{AB}, \rho_{BC}$ (representing X, Y, Z in Figure 1) and POVMs $\mathcal{M}_A, \mathcal{M}_B, \mathcal{M}_C$ such that the joint quantum probability distribution (2) is not of the form (1).

The MTS is a fundamental example in quantum network studies, valuable for both practical applications (e.g., certifying quantum devices) and theoretical insights into quantum mechanics. As has been said, it is particularly interesting because while nonlocal distributions (compatible with relativistic no-signaling) have been found for the MTS (cf. [5]), whether these are quantum realizable is still unknown.

Let us begin by fixing some notation. Let $\mathcal{P}$ be the set of all joint probability distributions in the MTS, and $\mathcal{Q} \subset \mathcal{P}$ be the set of all quantum distributions as in (2). Similarly, let $\mathcal{L}$ be the set of all local distributions. A certificate of infeasibility is denoted by C. If $P \in \mathcal{P}$, the evaluation of certificate C on distribution P is written as $C[P]$. By definition, $C[P] < 0 \Rightarrow P \notin \mathcal{L}$.

Our original approach for finding a quantum nonlocal distribution is summarized Algorithm 1. The main idea is to generate a certificate of infeasibility from some random (not necessarily quantum-realizable) distribution. Once we have a certificate C, we try to find a *quantum* distribution P_Q for which nonlocality is proven, i.e. $C[P_Q] < 0$. If we fail, we move on to another randomly generated certificate. For this to work, the certificate should approximate the boundary between local and nonlocal phenomena for nonlocal points near this boundary. This is the subject of study in the next section.

[3] All code implementations are publicly available at https://github.com/mvinervi7/Triangle.git.

A. Contour lines of infeasability certificates

Consider the following family of distributions for the MTS,

$$P_G(p,q) = p\delta_{000} + q\delta_{111} + \frac{1-p-q}{6}\delta. \tag{6}$$

Where δ_{000} is the distribution with support only on the 000 event (analogously for δ_{111}), and δ contains equal probabilities on all other (non-000 and non-111) outcomes. Also, $p, q \in [0,1] = I$. A first observation is that $P_G(0,0)$ is local. Indeed, with notations as in Fig. 1, let X, Y, Z be 3 random numbers in I, with at least two different. The local strategy where each party outputs 1 if the input they receive from the left is strictly bigger than the one from the right, and 0 otherwise, realizes the probability distribution $P_G(0,0)$. It is also intuitively clear that $P_G(1/2,1/2)$ is nonlocal, with a proof in [7].

Now, to identify the nonlocal regions, we examine straight segments from $(0,0)$ to points in $\{(1,q) \mid 0 \leq q \leq 1\} \cup \{(p,1) \mid 0 \leq p \leq 1\}$. Using the bisection method, we identify the first *transition* point on each segment where inflation verifies that $P_G(p,q)$ is nonlocal. The blue dots in Figure 3 illustrate these results.

Next, we test how well the contour lines of a point's certificate near the boundary align with the actual boundary. Consider the segment $p = q$, parametrized as (t,t), $t \in I$. Using the bisection method, suppose that inflation first detects nonlocality for $t = t^*$. By setting $t = t^* + \varepsilon$ with $\varepsilon > 0$, we obtain a certificate of infeasibility due to inflation, C. In Fig. 3, $\varepsilon = 1 \times 10^{-4}$. Plotting the contour lines of $f(p,q) = C[P_G(p,q)]$, we see they align with the curve connecting all transition points, as we sought to prove.

As a final comment, we mentioned that certificates provide a separating *hyperplane*, where distributions on one side are nonlocal. However, the contour line $f(p,q) = 0$ is not straight because inflation examines marginal probabilities, which are polynomials of the original distribution. Consequently, while inequalities in the inflated subgraph are linear in the inflated distribution, they are polynomial in the original distribution.

B. MTS Code

In section III, we reviewed the code for finding a quantum nonlocal distribution in the MTS. A key aspect is parametrizing a reasonable subspace of $\mathcal{Q}$. We start with the code in [9] for parametrizing unitary matrices. Take notations as in Fig.1. Let X, Y, Z be systems of two (entangled) qubits. Then, if $\mathcal{H}_A$ is Alice's Hilbert space, $\dim(\mathcal{H}_A) = 4$, as it contains one qubit from X and one from Y. All states in $\mathcal{H}_A$ can be parametrized by applying a unitary operator $\hat{U}_s$ to a fixed state $|\phi_A\rangle$,"rotating" it into any other state.

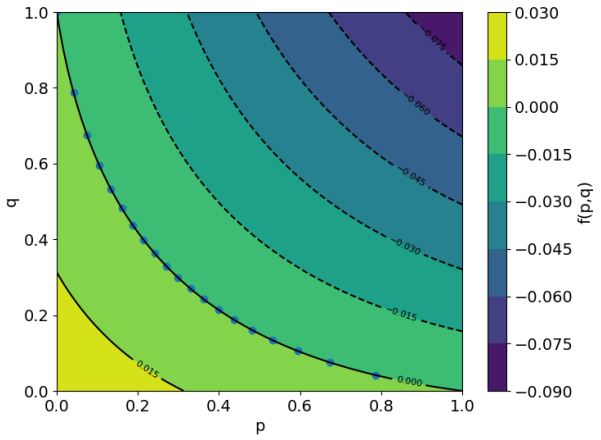

Figure 3: Contour lines and heat map of $f(p,q) = C[P_G(p,q)]$, for the certificate C corresponding to the point $\varepsilon = 1 \times 10^{-4}$ above the critical value on the segment $p = q$. Transition points obtained for different segments beginning at (0,0) are pictured with blue dots.

For measurements, take an orthonormal basis $|i\rangle, i = 0 \ldots 3$. For another unitary operator $\hat{U}_m$, consider projective measurements $\Pi_i = \hat{U}_m^\dagger |i\rangle \langle i| \hat{U}_m$, yielding 4 outcomes. To get binary outputs, introduce transition probabilities $p(a|i)$, $a \in 0, 1$, $i = 0, \ldots 3$, with $p(0|i) + p(1|i) = 1$. Define a POVM $P_{a=0} = \sum_{i=0}^{3} p(0|i)\Pi_i$, $P_{a=1} = \sum_{i=0}^{3} p(1|i)\Pi_i$. This parametrizes a subset of $\mathcal{Q}$ with pure states and coarse-grained projective measurements.

Choosing the minimization algorithm in Line 7 of Algoritm 1 is crucial. We explored different techniques and versions of the code:

1. Initially, we used the *Nelder-Mead* method from `scipy.optimize.minimize`. The main concern with this first version was the code's slowness.

2. Next, we implemented a gradient descent using the JAX library [11], speeding up execution and offering flexibility in epochs. However, evaluation time for certificates was a bottleneck.

3. An interesting approach was proposed in [8]. They explored 4884 inequalities for the MTS through an analysis of independence in the spiral inflation (Fig. 2a). These were refined to 52 equations in 4 groups, considering symmetry (a representative from each group is in the appendix). Instead of randomly selecting points outside the local set and extracting their certificates, we used gradient descent to minimize each chosen inequality (with 4 parallel gradient descents for independence). Using hard-coded inequalities instead of changing certificates reduced execution time, as symbolic evaluation of changing certificates was slow.

For this last version of the code, while extremely low values were recorded for some inequalities (around 1×10^{-7}), no quantum nonlocal distribution was found. Nevertheless, the code's efficient execution time and flexibility warrant promising alternatives to explore. One example would be considering entangled *qutrits* – instead of qubits – as quantum resources among parties. However, an implementation with higher dimensional systems raises efficiency and computer memory concerns that must be addressed in future research.

C. Beyond the MTS: 3 outcomes scenario

As mentioned above, an advantage of our code is that it is easily adaptable to scenarios related to the MTS. An example would be considering a scenario with 3 outcomes per party instead of 2. In this setting, we considered the family of *symmetric* distributions,

$$P(s_{111}, s_{112}, s_{123}) = \frac{s_{111}}{3}\delta_{\text{eq}} + \frac{s_{123}}{6}\delta_{\text{dif}} + \frac{s_{112}}{18}\delta$$

Where δ_{eq} is the flat distribution, with non-zero probabilities only if all three outcomes are the same, similarly δ_{dif} if all three outcomes are different, and δ for the rest of the events (two outcomes the same, one different). These distributions bear resemblance to the *Elegant Joint Measurement* distribution, a prime candidate for studying triangle nonlocality in the four-outcomes case [12]. To identify quantum nonlocal distributions, we employ gradient descent to minimize the Euclidean distance between each distribution $P(s_{111}, s_{112}, s_{123})$ for $0.36 \leq s_{111} \leq 0.48$. These bounds align with those in [10], where a similar approach is undertaken using neural networks to find local strategies yielding distributions close to points in this subspace. Results are presented in Fig. 4, and a table with all considered points can be found in the appendix.

The similarity of the figures suggests that, on average, there is no significant advantage when using qubits over classical models. However, for specific points like $(s_{111}, s_{112}, s_{123}) = (0.4, 0.32, 0.28)$, the quantum algorithm reduces the Euclidean distance by approximately 20%. This result motivates the exploration of entangled qutrits in place of qubits for future research. Employing qutrits could potentially yield even greater reductions in Euclidean distances for symmetric distributions, furthering the promise of this quantum algorithm.

IV. CONCLUSIONS

- In section III A, we attempted to study the relationship (for a particular family of distributions) between infeasability certificates and the boundary separating local from nonlocal behaviors. To do so, we saw how different nonlocal distributions – found by inflation – lied relative to a particular certificate, and found good agreement.

- Through parametrizing a subset of $\mathcal{Q}$ and minimizing certificates in multiple ways, we had aimed to find a quantum nonlocal distribution in the MTS. Even though extremely low values for certificates have been attained (near 1×10^{-7}) no such distributions have been found.

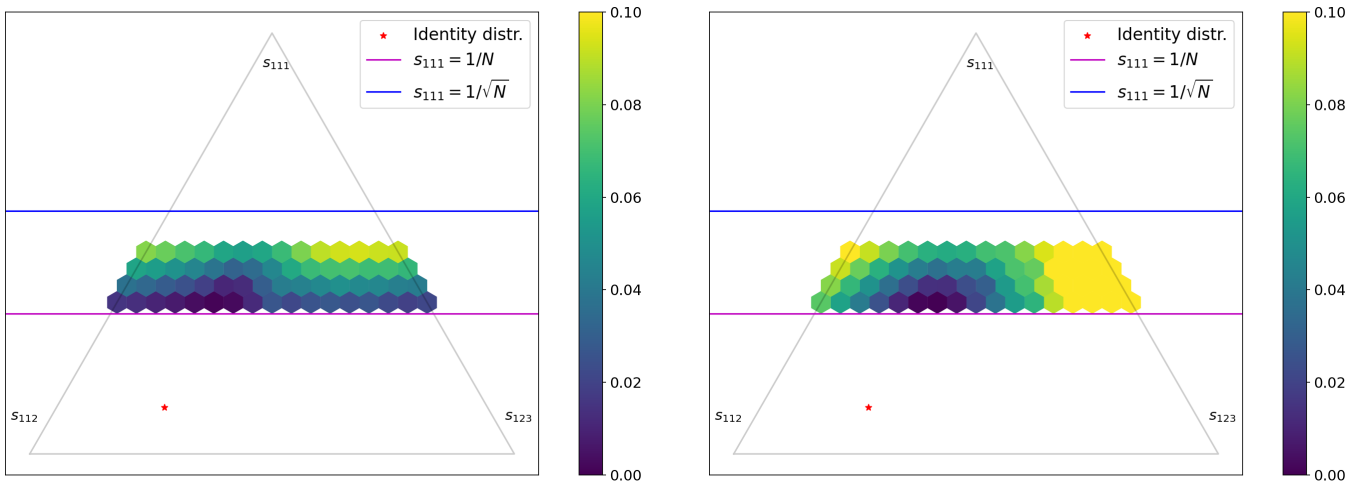

Figure 4: Ref. [10] results using neural networks to find classical models (a) versus ours using qubits (b). Colours are linked to Euclidean distances by the legends at the right of each plot. The three corners correspond to the three extremal distributions $s_{111} = 1$ (top), $s_{112} = 1$ (bottom left) and $s_{123} = 1$ (bottom right). The identity distribution $s_{111}/3 = s_{112}/18 = s_{123}/6$ is also plotted. In this same reference, it is shown that above the blue line no distributions can exist compatible with the triangle structure.

While computer memory concerns apply to higher dimensional systems, these promising outcomes serve as motivation to replicate the code with qutrits, rather than qubits, in future investigations.

- Generalizing further, we minimised the Euclidean distance between $\mathcal{Q}$ and different instances of symmetric distributions for the three outcomes scenario. Comparing our results to previous ones where only classical models were considered, we conclude that while there is no quantum advantage overall, there are specific distributions for which our implementation obtained appreciably better results (i.e., a decrease in 20% for the final Euclidean distance).

Acknowledgments

I would like to thank Emanuel-Cristian Boghiu, Tamás Kriváchy, and Bruno Julià-Díaz for their guidance and advice. Additionally, I am deeply grateful to ICFO and Antonio Acín for enabling me to conduct my thesis with the QIT group.

Finally, a warm thanks to my family for their unconditional support throughout.

[1] Bell, J. S. (1964). *On the Einstein Podolsky Rosen paradox*. Physics Physique Fizika, 1(3), 195–200.
[2] Tavakoli, A., Pozas-Kerstjens, A., Luo, M.-X., and Renou, M.-O. (2022). *Bell nonlocality in networks*. Reports on Progress in Physics, 85(5), 056001.
[3] Fritz, T. (2012). New Journal of Physics, 14, 103001.
[4] Cavalcanti, D. and Skrzypczyk, P. (2023). *Semidefinite Programming in Quantum Information Science*. IOP Publishing.
[5] Pozas-Kerstjens, A., Girardin, A., Kriváchy, T., Tavakoli, A., and Gisin, N. (2023). Post-quantum nonlocality in the minimal triangle scenario. arXiv:2305.03745 [quant-ph].
[6] Renou, M.-O., Trillo, D., Weilenmann, M., Le, T. P., Tavakoli, A., Gisin, N., Acín, A., and Navascués, M. (2021). Quantum theory based on real numbers can be experimentally falsified. *Nature*, 600(7890), 625-629.
[7] Boghiu, E.-C., Wolfe, E., Pozas-Kerstjens, A. (2022). *Inflation: a Python library for classical and quantum causal compatibility*. arXiv:2211.04483v2.
[8] Wolfe, E., Spekkens, R. W. and Fritz, T. (2019). The Inflation Technique for Causal Inference with Latent Variables. Journal of Causal Inference, 7(2), 1-15.
[9] Spengler, C., Huber, M., and Hiesmayr, B. C. (2010). A composite parameterization of unitary groups, density matrices and subspaces. Journal of Physics A: Mathematical and Theoretical, 43(38), 385306.
[10] Bäumer, E., Gitton, V., Kriváchy, T., Gisin, N., and Renner, R. (2024). *Exploring the Local Landscape in the Triangle Network*. arXiv:2405.08939 [quant-ph].
[11] James Bradbury, Roy Frostig. *JAX: composable transformations of Python+NumPy programs*. 2018. Version 0.3.13. Available online: http://github.com/google/jax.
[12] Gisin, N. (2017). The Elegant Joint Quantum Measurement and some conjectures about N-locality in the Triangle and other Configurations. *arXiv preprint* arXiv:1708.05556.

APPENDIX

A. Set of inequalities for the MTS

We now present the 52 inequalities mentioned in section III B, that can be found in [8]. They can be fit into 4 categories up to symmetry. A representative of each category is given below,

$$0 \leq 1 - \mathbb{E}[AC] - \mathbb{E}[BC] + \mathbb{E}[A]\mathbb{E}[B]$$

$$\begin{aligned} 0 \leq 3 &- \mathbb{E}[A] - \mathbb{E}[B] - \mathbb{E}[C] + 2\mathbb{E}[AB] + 2\mathbb{E}[AC] + 2\mathbb{E}[BC] \\ &+ \mathbb{E}[ABC] + \mathbb{E}[A]\mathbb{E}[B] + \mathbb{E}[A]\mathbb{E}[C] + \mathbb{E}[B]\mathbb{E}[C] \\ &- \mathbb{E}[A]\mathbb{E}[BC] - \mathbb{E}[B]\mathbb{E}[AC] - \mathbb{E}[C]\mathbb{E}[AB] \\ &+ \mathbb{E}[A]\mathbb{E}[B]\mathbb{E}[C] \end{aligned}$$

$$\begin{aligned} 0 \leq 4 &+ 2\mathbb{E}[C] - 2\mathbb{E}[AB] - 3\mathbb{E}[AC] - 2\mathbb{E}[BC] - \mathbb{E}[ABC] \\ &+ \mathbb{E}[A]\mathbb{E}[B]\mathbb{E}[C] + 2\mathbb{E}[A]\mathbb{E}[B] + \mathbb{E}[A]\mathbb{E}[C] \\ &- \mathbb{E}[A]\mathbb{E}[BC] - \mathbb{E}[C]\mathbb{E}[AB] \end{aligned}$$

$$\begin{aligned} 0 \leq 4 &- 2\mathbb{E}[AB] - 2\mathbb{E}[AC] - 2\mathbb{E}[BC] - \mathbb{E}[ABC] \\ &+ 2\mathbb{E}[A]\mathbb{E}[B] + 2\mathbb{E}[A]\mathbb{E}[C] + 2\mathbb{E}[B]\mathbb{E}[C] \\ &- \mathbb{E}[A]\mathbb{E}[BC] - \mathbb{E}[B]\mathbb{E}[AC] - \mathbb{E}[C]\mathbb{E}[AB] \end{aligned}$$

Where the outputs of the parties are taken to be $\{-1, 1\}$ for convenience and are expressed in terms of *correlators* $\mathbb{E}[\cdot]$ (see [2]). The number of equations in each class is (from top to bottom) $12, 8, 24$ and 8.

B. Euclidean Distances in the three-outcomes scenario

s_{111}	s_{112}	s_{123}	Classical	Quantum
0.36	0.00	0.64	2.14×10^{-2}	1.53×10^{-1}
0.36	0.04	0.60	1.94×10^{-2}	1.34×10^{-1}
0.36	0.08	0.56	2.26×10^{-2}	2.10×10^{-1}
0.36	0.12	0.52	2.67×10^{-2}	1.03×10^{-1}
0.36	0.16	0.48	2.45×10^{-2}	8.98×10^{-2}
0.36	0.20	0.44	2.71×10^{-2}	6.48×10^{-2}
0.36	0.24	0.40	2.61×10^{-2}	5.48×10^{-2}
0.36	0.28	0.36	2.19×10^{-2}	3.81×10^{-2}
0.36	0.32	0.32	2.66×10^{-2}	2.10×10^{-2}
0.36	0.36	0.28	1.18×10^{-2}	5.33×10^{-3}
0.36	0.40	0.24	2.73×10^{-3}	3.18×10^{-4}
0.36	0.44	0.20	8.94×10^{-4}	1.20×10^{-3}
0.36	0.48	0.16	3.29×10^{-3}	1.06×10^{-2}
0.36	0.52	0.12	7.08×10^{-3}	2.51×10^{-2}
0.36	0.56	0.08	9.80×10^{-3}	4.10×10^{-2}
0.36	0.60	0.04	1.33×10^{-2}	5.77×10^{-2}
0.36	0.64	0.00	1.54×10^{-2}	7.40×10^{-2}
0.40	0.00	0.60	4.16×10^{-2}	1.50×10^{-1}
0.40	0.04	0.56	4.29×10^{-2}	1.33×10^{-1}
0.40	0.08	0.52	4.62×10^{-2}	1.17×10^{-1}
0.40	0.12	0.48	4.69×10^{-2}	1.04×10^{-1}
0.40	0.16	0.44	4.98×10^{-2}	8.68×10^{-2}
0.40	0.20	0.40	4.65×10^{-2}	6.99×10^{-2}
0.40	0.24	0.36	4.37×10^{-2}	5.39×10^{-2}
0.40	0.28	0.32	4.19×10^{-2}	2.98×10^{-2}
0.40	0.32	0.28	2.96×10^{-2}	2.37×10^{-2}
0.40	0.36	0.24	1.24×10^{-2}	1.36×10^{-2}
0.40	0.40	0.20	1.06×10^{-2}	1.38×10^{-2}
0.40	0.44	0.16	1.88×10^{-2}	2.35×10^{-2}
0.40	0.48	0.12	2.46×10^{-2}	3.63×10^{-2}
0.40	0.52	0.08	2.88×10^{-2}	5.07×10^{-2}
0.40	0.56	0.04	3.33×10^{-2}	6.60×10^{-2}
0.40	0.60	0.00	3.72×10^{-2}	8.19×10^{-2}
0.44	0.00	0.56	6.61×10^{-2}	1.48×10^{-1}
0.44	0.04	0.52	6.88×10^{-2}	1.33×10^{-1}
0.44	0.08	0.48	6.86×10^{-2}	1.27×10^{-1}
0.44	0.12	0.44	7.07×10^{-2}	1.03×10^{-1}
0.44	0.16	0.40	7.00×10^{-2}	7.63×10^{-2}
0.44	0.20	0.36	6.78×10^{-2}	7.17×10^{-2}
0.44	0.24	0.32	6.04×10^{-2}	5.78×10^{-2}
0.44	0.28	0.28	4.62×10^{-2}	4.21×10^{-2}
0.44	0.32	0.24	3.48×10^{-2}	4.20×10^{-2}
0.44	0.36	0.20	3.16×10^{-2}	3.68×10^{-2}
0.44	0.40	0.16	3.85×10^{-2}	4.19×10^{-2}
0.44	0.44	0.12	4.57×10^{-2}	5.15×10^{-2}
0.44	0.48	0.08	5.04×10^{-2}	6.36×10^{-2}
0.44	0.52	0.04	5.53×10^{-2}	7.72×10^{-2}
0.44	0.56	0.00	5.83×10^{-2}	9.18×10^{-2}
0.48	0.00	0.52	9.16×10^{-2}	1.50×10^{-1}
0.48	0.04	0.48	9.19×10^{-2}	1.38×10^{-1}
0.48	0.08	0.44	9.35×10^{-2}	1.20×10^{-1}
0.48	0.12	0.40	9.28×10^{-2}	9.44×10^{-2}
0.48	0.16	0.36	9.01×10^{-2}	8.17×10^{-2}
0.48	0.20	0.32	8.01×10^{-2}	7.17×10^{-2}
0.48	0.24	0.28	6.79×10^{-2}	6.98×10^{-2}
0.48	0.28	0.24	5.92×10^{-2}	6.32×10^{-2}
0.48	0.32	0.20	5.59×10^{-2}	6.10×10^{-2}
0.48	0.36	0.16	5.87×10^{-2}	6.35×10^{-2}
0.48	0.40	0.12	6.65×10^{-2}	7.01×10^{-2}
0.48	0.44	0.08	7.14×10^{-2}	7.97×10^{-2}
0.48	0.48	0.04	7.72×10^{-2}	9.13×10^{-2}
0.48	0.52	0.00	8.16×10^{-2}	1.04×10^{-1}

Table I: Table containing the final Euclidean distance obtained for the classical strategy proposed in [10] ('Classical') and for our qubit algorithm ('Quantum') for all setups $s_{111}, s_{112}, s_{123}$ considered in Fig. 4.